Viscosity Solutions and Convergence of Monotone Schemes for Synthetic Aperture Radar Shape-From-Shading Equations with Discontinuous Intensities

Daniel N. Ostrov
Department of Mathematics
Santa Clara University
Santa Clara, CA 95053

September 2, 1997

Abstract

The Shape-From-Shading equation relating $u(y, r)$, the unknown (angular) height of a surface, to $I(y, r)$, the known Synthetic Aperture Radar intensity data from the surface, is

$$I = \frac{u_r^2}{\sqrt{1 + u_r^2 + u_y^2}},$$

where y and r are axial and radial cylindrical coordinates. Unlike the more common eikonal Shape-From-Shading equation needed to relate surface height in Cartesian coordinates to optical/photographic intensity data, the above radar equation can be transformed into Hamilton-Jacobi Cauchy form: $u_r + g(I, u_y) = 0$. We explore the case where I is a discontinuous function, which occurs commonly in radar data. By considering sequences of continuous intensity functions that converge to I, we obtain corresponding sequences of viscosity solutions. We prove that these sequences must converge. We also establish conditions that guarantee that these sequences converge to a common limit, which we define as the solution to the radar equation. Finally, we establish and demonstrate that when this common limit exists, monotone numerical schemes must converge to this solution as the mesh size decreases.

1 Introduction

The goal of Shape-From-Shading (SFS) is to reconstruct the shape (topography) of a 3-D surface by exploiting a 2-D image of the surface. A typical example of SFS is attempting to reconstruct a 3-D surface by using a photograph of the surface, which is an issue of interest in the field of machine vision. A less intuitive — though extremely common — example of SFS is attempting to reconstruct a 3-D surface from a radar image of the surface. Synthetic Aperture Radar (SAR) is a widely used radar imaging method, and there is much interest in using SAR data to determine the 3-D shapes of objects. For example, the 1990 Magellan Space Probe collected high resolution SAR data for most of the Venusian surface, so progress in the SAR SFS problem can enable the determination of a more detailed mapping of the topography of Venus.

Although the equations for machine vision SFS (which will be referred to as "optical SFS" throughout this article) are related to the equations for SAR SFS, the equations are not identical. Optical SFS equations are Hamilton-Jacobi equations that generally require Dirichlet boundary conditions, whereas SAR SFS equations can be transformed into Hamilton-Jacobi equations requiring only Cauchy boundary conditions [1]. For both cases, solving the equation requires knowing the albedo (the "whiteness") of the surface and also the surface reflectance properties (the "texture"). We will assume these are known. We will also assume that the surface is non-self occluding (i.e., contains no shadows).

The *intensity function*, $I(\cdot, \cdot)$, describes the information of the 2-D image. In the optical SFS case, the intensity function represents the brightness at each pixel point in a black and white photograph from a camera equipped with a flash. In the SAR SFS case, the intensity represents the density of radar signals returned to a satellite as opposed to the density of light photons returned to a camera lens. When the intensity function is continuous and appropriate boundary conditions are specified, it is known that a unique viscosity solution (3-D topography) exists in both the optical and SAR SFS problems. When the intensity is discontinuous, however, there has only been partial progress in resolving the uniqueness question for the optical SFS equations and there has been no work for the SAR SFS equation.

In this paper we explore the problem of SAR SFS when the intensity function is discontinuous. By exploiting the physical properties of SAR, we will establish that a unique solution often exists even when the intensity is discontinuous. We will also prove that monotone numerical schemes, which can be used to construct viscosity solutions when the intensity is continuous, can also be used to construct this discontinuous intensity solution.

The organization of this paper is as follows: In the next section, we explore the history and recent developments in optical SFS problems and SAR SFS problems. In the third section, we will derive the Cauchy form of the SAR SFS Hamilton-Jacobi equation. In section four, we will discuss the relevant physical constraints on SAR which we will use to establish two appropriate sequences of approximate solutions. In section five, we prove a monotonicity result which establishes the existence of the limits of these two sequences,

which we will label the upper solution and the lower solution, and we examine when the upper and lower solution coincide, which defines a unique solution. Finally, in section six we establish that when the upper and lower solution coincide, monotone numerical schemes must converge to this unique common solution and we present some numerical examples of surface reconstructions from discontinuous intensity functions.

2 Previous work on the Shape-From-Shading Problem

Most theoretical work in SFS has been performed on the optical SFS problem. We consider the specific case of optical SFS where the only light source is far away from the surface of interest and the recording device (e.g., the camera or eye) views the surface at the same angle as the incident light.

Since the albedo of the surface is assumed to be known, its effect in the optical SFS equation can be completely compensated, therefore albedo does not appear in our final equation. Also, we assume that the surface is Lambertian, i.e., incident light rays are reflected equally in all directions by the surface. We define the z axis to correspond to the direction of the light rays, $Z(x, y)$ to be the unknown height of the surface (where x and y are the Cartesian coordinates perpendicular to z), and $I(x, y)$ to be the known light intensity (e.g. photo brightness). Under the above assumptions, the intensity is merely the cosine of the angle between the surface normal and the z-axis, which can be expressed in terms of the partial derivatives of Z by

$$I(x, y) = \frac{1}{\sqrt{1 + Z_x^2 + Z_y^2}}. \tag{2.1}$$

This eikonal equation is the *optical SFS equation*.

Since the characteristic curves for eq (2.1), examined by Horn and others in the 1970's [2], flow in the direction of the gradient of Z, information collects at the critical points (i.e., (x, y) locations where $\nabla Z = 0$ and $I = 1$). Recently Dupuis and Oliensis [3] used this convergence of information at critical points to show that if $Z(x, y)$ is C^2 and there are a finite, non-zero number of critical points in the intensity data, then knowledge of the height at a single critical point where it is known that the critical point is a local maximum of the surface (or minimum) can be used to determine most of the surface $Z(x, y)$. If we cannot assume $Z(x, y)$ is C^2, then we require more conditions to establish uniqueness. In 1992 Rouy and Tourin [4] determined that eq (2.1) has a unique continuous — though possibly nonsmooth — viscosity solution [5,6] if I is continuous and we know the height at all of the critical points and along the boundary of a Lipschitz continuous intensity function's domain (i.e., Dirichlet boundary conditions). (When shadows are present, other conditions are used, as discussed in [7].) Typically, nonsmooth surfaces correspond to discontinuous intensities, but many questions remain as to whether a unique viscosity solution exists for the optical SFS equation when the intensity function is discontinuous. In 1991 Tourin [8]

made some progress on this question by applying an extension of the notion of viscosity solutions developed by Ishii [9] for discontinuous Hamiltonians to some very specific cases of the discontinuous optical SFS problem.

The study of Synthetic Aperture Radar SFS has generally been tied to analyses of optical SFS. Although there are connections between the two problems, there are also significant differences, as discussed in [1] and summarized in the next section. For example, a useful intensity function $I(y, r)$ for SAR contains *no* critical points, so it is impossible to uniquely reconstruct $u(y, r)$, the function describing surface "height" from SAR data, using information from a single point on the surface, even if we know that $u(y, r)$ is C^2. Further, we can transform the partial differential equation that relates u and I for SAR SFS, i.e.,

$$I(y, r) = \frac{u_r^2}{\sqrt{1 + u_r^2 + u_y^2}}, \tag{2.2}$$

into an evolution-like Hamilton-Jacobi form

$$u_r - I\sqrt{.5 + \sqrt{.25 + (1 + u_y^2)/I^2}} = 0, \tag{2.3}$$

therefore it is clear that Cauchy – as opposed to Dirichlet – boundary conditions are appropriate. From Souganidis [10], following from Crandall, Lions, and Evans in [5] and [6], we can show that when both the intensity and the Cauchy boundary conditions are bounded Lipschitz functions, a unique viscosity solution, which is bounded and Lipschitz continuous, exists for eq (2.3). Further, Souganidis [11], expanding on numerical work by Crandall and Lions in [12], has also shown that any monotone finite difference evolution scheme must converge to this unique viscosity solution.

Before analyzing the case where the intensity function is discontinuous, we discuss the physical background and derivation of eq (2.3), the SAR SFS equation, in the next section.

3 Hamilton-Jacobi Model of Synthetic Aperture Radar

SAR radar pictures are usually taken by satellites moving (approximately) linearly at constant velocity high above a surface (see fig. 1). We define the linear path of the satellite to be the y axis. The radar signal sent from the satellite is at an angle, φ, with the vertical direction. In practice φ is essentially constant since the satellite is far from the surface.

Each time the satellite progresses some fixed amount in y it sends a burst of radar signals (over some short time interval) down to the surface. The satellite records both the return times of the radar signals in the burst and the intensity of the returned signals. The return time corresponds to the radial distance of the surface from the satellite. By combining and filtering information from all the bursts, the locally averaged radar intensity for a Cartesian grid of (y, r) points on the surface is reported, where r is the distance between a point on the

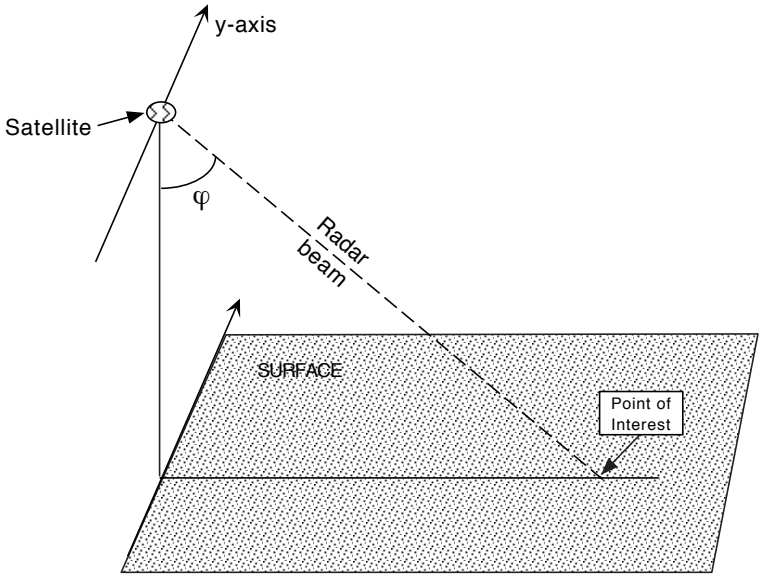

Figure 1: *Satellite transmission of Synthetic Aperture Radar signals. The satellite moves parallel to the ground in the y direction. The radar signal is sent perpendicular to the y direction at an angle φ with the vertical direction.*

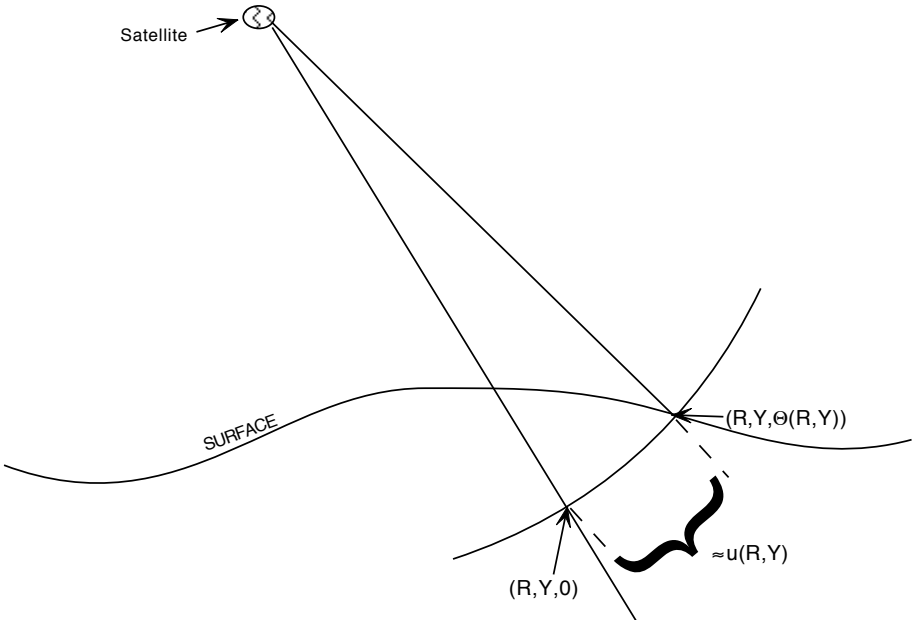

Figure 2: *Meaning of $u(r, y)$. We consider the cross-section of the surface where $y = Y$. Since r varies only a small amount over the range of collected intensity data, we can think of $u(R, Y)$ as the arclength of the subsection of the circle of radius R centered at the satellite that lies between the reference plane $\Theta = 0$ and the surface.*

surface and the y-axis. Normally, the (y, r) grid is small enough for us to closely approximate the actual intensity function.

Since the intensity function is parameterized by the y and r values corresponding to a surface location, we also wish to describe the height of the surface as a function parameterized by y and r. Because y and r are the axial and radial coordinates of a cylindrical coordinate system, we describe the surface height in terms of the angular coordinate θ. Specifically, we define the surface height function

$$u(y, r) \equiv r_0 \Theta(y, r),$$

where $\Theta(y, r)$ is the θ coordinate of a surface location whose other two coordinates are y and r, and r_0 is the average distance between the satellite and the surface. Because, in practice, the distance between the satellite and the surface is much larger than the range of r values in the data, $r \doteq r_0$, so $u(y, r)$ is approximately the length of the arc, for fixed y and r, that connects the surface to the (arbitrary) reference plane $\theta = 0$ (see fig. 2).

We next relate the intensity function, $I(y, r)$, to the surface function $u(y, r)$. The intensity function is a scaled ratio between P_s, the power per unit area of the transmitted satellite radar beam, which is constant, and $P_r(y, r)$, the returned power to the satellite from the

surface section near $(y, r, \Theta(y, r))$. We begin by relating P_s and $P_r(y, r)$ to $P_i(y, r)$, the incident power of the radar per unit area of actual surface.

Define ϕ to be the angle between the unit surface normal and the unit vector pointing from the surface to the satellite. The radar power density on the surface, P_i, is the projection of P_s, the constant power density of the radar, onto the actual surface:

$$P_i = P_s \cos(\phi). \tag{3.1}$$

As an analogy, one can think of P_s as the brightness of a flashlight and P_i as the number of photons striking per unit area of the surface upon which the flashlight shines. A simple geometric argument allows us to express $\cos(\phi)$ in terms of the partial derivatives of u:

$$\cos(\phi) = \frac{u_r}{\sqrt{1 + u_r^2 + u_y^2}}. \tag{3.2}$$

Just as in the case of optical SFS, we assume that the albedo of the surface is known, and therefore its effect can be compensated. In other words, without loss of generality we assume a unit albedo, which means that all the radar waves entering the surface are reflected by the surface (i.e., the surface is perfectly "white"). If the surface is Lambertian (i.e., the radar waves are reflected equally in all directions from the surface), then the power returned to the satellite associated to the grid point (y_i, r_j) is approximately proportional to $P_i(y_i, r_j)$, the incident power density at that point, multiplied by the differential area of the surface, ΔS, projected in the direction of the radar signal (and return), which is $\Delta u \Delta y$ (i. e., $\Delta u \Delta y = \Delta S \cos(\phi)$). Therefore,

$$P_r(y_i, r_j) \doteq k P_i(y_i, r_j) \Delta u \Delta y. \tag{3.3}$$

However, since each of the grid points in the intensity represents a $\Delta y \Delta r$ section of the surface, we must rewrite eq (3.3) in terms of Δy and Δr:

$$P_r(y_i, r_j) \doteq k P_i(y_i, r_j) u_r(y_i, r_j) \Delta y \Delta r. \tag{3.4}$$

Combining eqs (3.1), (3.2), and (3.4) yields

$$I(y_i, r_j) \equiv \frac{P_r}{k_2 P_s \Delta y \Delta r} = \frac{u_r^2(y_i, r_j)}{\sqrt{1 + u_r^2(y_i, r_j) + u_y^2(y_i, r_j)}}, \tag{3.5}$$

and the continuous analog of eq (3.5) is the SAR SFS equation that we seek:

$$I(y, r) = \frac{u_r^2}{\sqrt{1 + u_r^2 + u_y^2}}. \tag{3.6}$$

Although this paper will concentrate on Lambertian surfaces because of their wide application and relative simplicity, the results of this paper will also be applicable to non-Lambertian surfaces. (E. g., the surface of Venus is non-Lambertian due to the long wavelength of the radar utilized by Magellan to penetrate Venus's clouds). The non-Lambertian

case requires a slightly more sophisticated view of the Lambertian analysis. Replacing $\Delta u \Delta y$ with $\Delta S \cos(\phi)$ in eq (3.3) we have

$$P_r \doteq k P_i \cos(\phi) \Delta S. \tag{3.7}$$

where $\Delta S \doteq \sqrt{1 + u_r^2 + u_y^2} \Delta y \Delta r$. When the surface is not Lambertian, the $\cos(\phi)$ term in eq (3.7) can be modeled by $\cos^k(\phi)$, where k becomes larger as the surface becomes more reflective (mirrorlike). Applying eq (3.2) with the definition of the intensity in eq (3.5) leads to the continuous form of the non-Lambertian SAR SFS equation:

$$I(y, r) = \left(\frac{u_r}{\sqrt{1 + u_r^2 + u_y^2}} \right)^k u_r, \tag{3.8}$$

where $k \geq 1$.

We wish to note two important physical restrictions on the variables in eq (3.6) (and eq (3.8)). If, for a fixed value of y, the radial distance from the satellite to two different points on the surface is the same, the intensity data for this (y, r) value will correspond to the radar returned by *two* points on the surface. We exclude cases where this undesirable double exposure effect, commonly referred to as "layover", occurs by assuming that $u(y, r)$ is Lipschitz continuous, which implies that u_r cannot become infinitely large so I cannot become infinitely large and $\phi \neq 0$.

The radar beam is projected toward the surface at an angle — as opposed to downward — to avoid layover; however, if the angle of the projected radar beam becomes too steep, we get radar "shadows" (which are completely analogous to light shadows), and we get holes in our intensity data. (In other words we have no intensity values for (y, r) points associated with occluded sections of the surface). We assume that our intensity functions do not have shadows, and therefore are defined for all (y, r) of interest. As part of this requirement, we assume that $u_r > 0$, since — except in singular cases — $u_r = 0$ implies that we are on the boundary of a shadow region and $u_r < 0$ implies that we are inside a shadow region.

Note 1: We are assuming here that $\varphi > 0$; if $\varphi < 0$ then we merely replace the condition $u_r > 0$ with the condition $u_r < 0$.)

Note 2: Since we have assumed u is Lipschitz, u_y (when it exists) must be bounded, therefore the condition $u_r > 0$ also implies that $I > 0$. We will further assume that I does not get arbitrarily close to 0.

The physical restriction $u_r > 0$ causes most of the significant differences between the behavior of solutions of the optical SFS equation, eq (2.1), and of the SAR SFS equation, eq (3.6). For example, the characteristic curves $(Y(s), R(s))$ for eq (3.6) are governed by the characteristic equations:

$$\begin{aligned} \frac{dY}{ds} &= -2I^2 u_y \\ \frac{dR}{ds} &= 4u_r^3 - 2I^2 u_r. \end{aligned} \tag{3.9}$$

Since we can quickly establish that $4u_r^2 - 2I^2 > 0$, it is clear from eq (3.9) that when $u(y,r)$ is C^2, the flow established by the characteristic curves has *no* critical points since $u_r > 0$. Further, we have that $\frac{dR}{ds}$ is always positive, and therefore information always propagates in the direction of increasing r. This suggests algebraically transforming eq (3.6) to the evolution-type form

$$u_r - I\sqrt{.5 + \sqrt{.25 + (1 + u_y^2)/I^2}} = 0, \tag{3.10}$$

which again is possible only because we know that $u_r > 0$. Equations of this form usually describe the evolution of a solution with time. Here, however, we can think of r as time since information about the solution propagates with increasing r.

From viscosity solution theory, we can establish that eq (3.10) has a unique (bounded Lipschitz) viscosity solution if bounded Lipschitz Cauchy conditions are specified and $I(y,r)$ is Lipschitz (see section 5). Is it possible that the actual surface corresponds to a nonviscosity solution? Yes, but it is extremely unlikely. Since — except in singular cases — nonsmooth surfaces lead to discontinuous intensities, a continuous intensity will generally correspond to a smooth surface. When the surface is smooth, it will also be the unique viscosity solution, since a classical (i.e., smooth) solution is always a viscosity solution. Even in the unlikely event that the intensity is continuous but the viscosity solution (and therefore the actual surface) is not smooth, the fact that the viscosity solution minimizes the measure of the subset of the domain where the surface is not smooth still makes it a likely candidate to correspond to the actual surface. The selection of a solution with the most smoothness is common in topographical reconstruction, especially since there are no other physical criteria (like entropy) that can be exploited. For example, the most widely used methods for surface reconstruction when the intensity data is noisy rely on minimizing a cost functional based on fidelity to the intensity data and smoothness of the solution; since we assume there is no noise in the intensity here, this method reduces to selecting the most smooth solution. Because when $I(y,r)$ is continuous it is so unlikely that nonviscosity solutions correspond to the actual surface, we will only consider the viscosity solution from now on for continuous $I(y,r)$. With this in mind, we now proceed to the case where $I(y,r)$ is discontinuous.

4 Definition of a Solution when the Intensity Function is Discontinuous

We consider any intensity function $I(y,r)$ that is (1) bounded away from zero and infinity so that neither layover nor shadows can occur and (2) defined and continuous almost everywhere in the domain $\{(y,r)|y \in (-\infty,\infty), r \in [R_1,R_2]\}$. (Realistically, of course, y is contained in some finite interval. We differ discussion of that case for now.) On the set of points of discontinuity (which typically consists of a set of curves in the domain), the intensity function has no physical definition, but, for the moment, we define the intensity at any point

of discontinuity $x \equiv (y, r)$ by

$$I(x) = \limsup_{\xi \to x} I(\xi). \tag{4.1}$$

(Later, we will make use of the lower limit function, $\liminf_{\xi \to x} I(\xi)$, instead.) We wish to take advantage of our physical knowledge of SAR to define the appropriate notion of a unique solution of eq (3.10) using the intensity function defined in eq (4.1). From the previous section, we know that the intensity functions derived from radar information require local averaging of the actual intensity function for the surface. As the radar resolution improves, this local neighborhood shrinks. This suggests we consider the approximate solutions corresponding to approximate intensity functions where the value assigned to the approximate intensity at any point x is determined by utilizing the values of the actual intensity function throughout a small neighborhood of x. Our notion of a solution, therefore, must be the limit of these approximate solutions as the size of this neighborhood shrinks to zero. If this notion of solution were not to correspond to the actual physical surface, then it would be impossible to use radar to accurately reconstruct any surface whether the underlying intensity was continuous or discontinuous.

Even without a radar perspective, one would still think of the intensity function as a local average since the concept of an intensity function that is continuous almost everywhere requires a macroscopic idealization of the surface that is an average of the thoroughly discontinuous microscopic behavior of the planet surface.

With this view in mind, we now define specific approximate intensity functions, $I^\varepsilon(x)$, by

$$I^\varepsilon(x) = \sup_{\xi} \left(I(\xi) - \frac{1}{\varepsilon} |x - \xi| \right) \tag{4.2}$$

where $|x - \xi|$ is the Euclidean distance between the points x and ξ. $I^\varepsilon(x)$ can be described as the surface created by letting cones of slope $\frac{1}{\varepsilon}$ radiate downward from every point of the surface $I(x)$.

Since $I(x)$ cannot become infinitely large, $I^\varepsilon(x)$ can only depend on the value of I in a local neighborhood of x, therefore $I^\varepsilon(x)$ satisfies our physical requirements for approximate intensity functions. We wish to note three other properties of $I^\varepsilon(x)$ that are easy to establish:

Property 4.1: $I^\varepsilon(x)$ is Lipschitz continuous with Lipschitz constant $\frac{1}{\varepsilon}$.
Property 4.2: $\varepsilon_1 \geq \varepsilon_2 \Rightarrow I^{\varepsilon_1}(x) \geq I^{\varepsilon_2}(x) \quad \forall x$.
Property 4.3: $\lim_{\varepsilon \to 0} I^\varepsilon(x) = I(x) \quad \forall x$.

The last of these three properties is due to the definition of the intensity function made in eq (4.1). We choose the specific form of $I^\varepsilon(x)$ in eq (4.2) because of property 2, which states that for any fixed x, $I^\varepsilon(x)$ monotonically decreases as ε decreases. This property will be crucial in the next section, where we show that $u^\varepsilon(x)$, the viscosity solutions that correspond to the continuous approximate intensities, must converge as $\varepsilon \to 0$.

5 Uniqueness of the Limit of Approximate Solutions for a Discontinuous Intensity Function

We begin by defining the open domain $\Omega \equiv \{(y,r)|y \in (-\infty,\infty), r \in (R_1,R_2)\}$ and the domain of the solution $\Omega' \equiv \Omega \bigcup \{(y,R_2)|y \in (-\infty,\infty)\}$. We assume that boundary conditions are known; that is, the value of u is known at $r = R_1$ (or, alternatively, we could have conditions at $r = R_2$ specified.) We refer the reader to [1] for some methods of obtaining this boundary data.

We now recall a definition due to Crandall, Lions, and Evans in [5,6] and a uniqueness and existence theorem due to Souganidis in [10] for viscosity solutions:

Definition (Viscosity solution): A function $u \in C(\overline{\Omega})$ is a *viscosity solution* of an equation of the form $u_r(x) + H(x, u_y(x)) = 0$ if for any (smooth) function $\phi \in C^1(\Omega')$, we have that
(a) At any point $x_0 \in \Omega'$ where $u(x) - \phi(x)$ attains a local maximum, we have that $\phi_r(x_0) + H(x_0, \phi_y(x_0)) \leq 0$,
and
(b) At any point $x_0 \in \Omega'$ where $u(x) - \phi(x)$ attains a local minimum, we have that $\phi_r(x_0) + H(x_0, \phi_y(x_0)) \geq 0$.

Theorem A (Uniqueness and Existence for a Continuous Hamiltonian): If, $\forall x \in C(\overline{\Omega})$, (1) $H(x, u_y)$ is uniformly continuous in x and u_y, (2) $\sup_x |H(x,0)| < \infty$, (3) There exists a C such that $|H(x,u_y) - H(\xi,u_y)| \leq C(1+|u_y|)|x-\xi|$, and (4) the boundary condition at $r = R_1$ is a bounded Lipschitz function, then the equation $u_r + H(x,u_y) = 0$
(1) has a unique viscosity solution satisfying the boundary condition at $r = R_1$ and
(2) this viscosity solution is a bounded Lipschitz function on $\overline{\Omega}$.

Before applying Theorem A to the case of the approximate intensities, I^ε, we express eq (3.10), the SAR SFS equation, as

$$u_r + g(I(x), u_y) = 0,$$

$$\text{where } g(I(x),u_y) = H(x,u_y) = -I(x)\sqrt{.5 + \sqrt{.25 + (1+u_y^2)/I^2(x)}}, \tag{5.1}$$

and note two important properties of the function $g(I, u_y)$:
Property 5.1: $\frac{\partial g}{\partial u_y}$ is continuous and $\left|\frac{\partial g}{\partial u_y}\right| < \frac{1}{2}$.
Property 5.2: $\frac{\partial g}{\partial I}$ is continuous and $\frac{\partial g}{\partial I} < 0$.
We now establish that a unique bounded Lipschitz viscosity solution, u^ε, exists for $u_r + g(I^\varepsilon(x), u_y) = 0$ where — regardless of the value of ε — the actual surface values at $r = R_1$ are used for boundary conditions. Recalling from property 4.1 that I^ε is Lipschitz, we know from the continuity of the partial derivatives in property 5.1 and 5.2 that $H^\varepsilon(x,u_y)(\equiv g(I^\varepsilon(x),u_y))$ is uniformly continuous in x and u_y. Further, since $I(x)$ is a positive bounded function, I^ε must also be a positive bounded function, therefore $\sup_x |H^\varepsilon(x,0)|$ must be finite. We can satisfy condition (3) of the uniqueness/existence theorem by showing that

$\left|\frac{\partial H^\varepsilon}{\partial x}\right| = \left|\frac{\partial g}{\partial I^\varepsilon}\right| \left|\frac{\partial I^\varepsilon}{\partial x}\right| \leq C\left(1 + \left|u_y^\varepsilon\right|\right)$. This follows since I^ε is Lipschitz and bounded away from 0 and ∞, which implies that $\left|\frac{\partial I^\varepsilon}{\partial x}\right|$ is bounded and $\left|\frac{\partial g}{\partial I^\varepsilon}\right| \leq C\left(1 + \left|u_y^\varepsilon\right|^{\frac{3}{4}}\right)$. Finally, since the actual surface is assumed to be Lipschitz, the boundary condition must be Lipschitz, and since the range of y is finite in any realistic situation, we can assume this boundary condition is a bounded function without requiring new physical assumptions. Therefore, for any fixed ε, the uniqueness and existence theorem establishes that u^ε, the unique viscosity solution, is a bounded, Lipschitz function.

With this in mind, we now present a theorem, based on the uniqueness argument for viscosity solutions in [13], which exploits the monotonic dependence of g on I in property 5.2 to establish that the u^ε functions are monotonic:

Theorem 5.1 *(monotonicity): If $\varepsilon_1 > \varepsilon_2$ then $u^{\varepsilon_1}(y,r) \geq u^{\varepsilon_2}(y,r)\ \forall (y,r) \in \overline{\Omega}$.*

Proof: Assume that the theorem is false, therefore

$$\sup_{\bar{\Omega}} \left(u^{\varepsilon_2} - u^{\varepsilon_1}\right) = \sigma > 0. \tag{5.2}$$

Choose $\epsilon > 0$, $0 < \lambda < 1$, and define

$$\Phi(y,z,r,s) \equiv u^{\varepsilon_2}(y,r) - u^{\varepsilon_1}(z,s) - \lambda(r+s) - \frac{1}{\epsilon^2}\left((y-z)^2 + (r-s)^2\right), \tag{5.3}$$

where $y, z \in (-\infty, \infty)$ and $r, s \geq R_1$. Now choose $0 < \delta < 1$ and select a point $(y_0, z_0, r_0, s_0) \in (-\infty,\infty)^2 \times [R_1, R_2]^2$ with

$$\Phi(y_0,z_0,r_0,s_0) \geq \sup_{\bar{\Omega}\times\bar{\Omega}} \Phi(y,z,r,s) - \delta. \tag{5.4}$$

According to eq (5.2) we have

$$\Phi(y_0,z_0,r_0,s_0) \geq \sup_{\bar{\Omega}} \Phi(y,y,r,r) - \delta \geq \sigma - 2\lambda R_2 - \delta, \tag{5.5}$$

and from eq (5.3) we see that

$$\frac{1}{\epsilon^2}\left((y_0-z_0)^2 + (r_0-s_0)^2\right) \leq 2\lambda(R_2 - R_1) + \delta + u^{\varepsilon_2}(y_0,r_0) - u^{\varepsilon_1}(z_0,s_0) - \sigma. \tag{5.6}$$

Since u^{ε_1} and u^{ε_2} are bounded, we have that

$$\sqrt{(y_0-z_0)^2 + (r_0-s_0)^2} = O(\epsilon).$$

Next we define C^{ε_1} to denote the Lipschitz constant of u^{ε_1} and C^{ε_2} to denote the Lipschitz constant of u^{ε_2}; i. e.,

$$|u^{\varepsilon_1}(y,r) - u^{\varepsilon_1}(z,s)| \leq C^{\varepsilon_1}\sqrt{(y-z)^2 + (r-s)^2} \tag{5.7a}$$

$$|u^{\varepsilon_2}(y,r) - u^{\varepsilon_2}(z,s)| \leq C^{\varepsilon_2}\sqrt{(y-z)^2 + (r-s)^2}, \tag{5.7b}$$

where $y, z \in (-\infty, \infty)$ and $r, s \in [R_1, R_2]$.

Now choose $\lambda, \delta > 0$ so that $2\lambda R_2 + \delta < \frac{\sigma}{2}$, so from the fact that $\sqrt{(y_0 - z_0)^2 + (r_0 - s_0)^2} = O(\epsilon)$ and the initial condition we see that

$$\begin{aligned}
\frac{\sigma}{2} &\leq u^{\varepsilon_2}(y_0, r_0) - u^{\varepsilon_1}(z_0, s_0) \\
&= u^{\varepsilon_2}(y_0, r_0) - u^{\varepsilon_2}(y_0, R_1) + u^{\varepsilon_2}(y_0, R_1) - u^{\varepsilon_1}(y_0, R_1) \\
&\qquad + u^{\varepsilon_1}(y_0, R_1) - u^{\varepsilon_1}(y_0, r_0) + u^{\varepsilon_1}(y_0, r_0) - u^{\varepsilon_1}(z_0, s_0) \\
&\leq C^{\varepsilon_2}(r_0 - R_1) + C^{\varepsilon_1}(r_0 - R_1) \pm C^{\varepsilon_1}(O(\epsilon)).
\end{aligned} \tag{5.8}$$

Now select $\epsilon > 0$ to be so small that $\frac{\sigma}{4} \leq C^{\varepsilon_2}(r_0 - R_1) + C^{\varepsilon_1}(r_0 - R_1)$, which implies that for some constant $\mu > 0$, we have that $(r_0 - R_1) \geq \mu > 0$. A similar argument establishes that $(s_0 - R_1) \geq \mu > 0$.

Next we define a smooth cutoff function $\zeta(y, z, r, s)$ with the properties $\zeta \in [0, 1]$, $\zeta(y_0, z_0, r_0, s_0) = 1$, and $\zeta(y, z, r, s) = 0$ if $(y - y_0)^2 + (z - z_0)^2 + (r - r_0)^2 + (s - s_0)^2 > \mu^2/4$. We also define

$$\Psi(y, z, r, s) \equiv \Phi(y, z, r, s) + 2\delta\zeta(y, z, r, s). \tag{5.9}$$

Since $\Psi = \Phi$ off the support of ζ, but (from eq (5.4))

$$\Psi(y_0, z_0, r_0, s_0) = \Phi(y_0, z_0, r_0, s_0) + 2\delta > \sup_{\bar{\Omega} \times \bar{\Omega}} \Phi + \delta, \tag{5.10}$$

we see that Ψ attains its maximum over $(-\infty, \infty)^2 \times [R_1, R_2]^2$ at some point (y_1, z_1, r_1, s_1) contained in the support of ζ. In particular we have that $r_1, s_1 > \mu/2 + R_1$.

Now observe that the mapping $(y, r) \mapsto \Psi(y, z_1, r, s_1)$ has a maximum at the point (y_1, r_1). Applying eq (5.3) and eq (5.9) we see that $u^{\varepsilon_2} - v$ has a maximum at (y_1, r_1) where v is defined by

$$v(y, r) \equiv u^{\varepsilon_1}(z_1, s_1) + \lambda(r + s_1) + \frac{1}{\epsilon^2}\left((y - z_1)^2 + (r - s_1)^2\right) - 2\delta\zeta(y, z_1, r, s_1). \tag{5.11}$$

Since u^{ε_2} is a viscosity solution,

$$v_r(y_1, r_1) + g\left(I^{\varepsilon_2}(y_1, r_1), v_y(y_1, r_1)\right) \leq 0;$$

that is,

$$\begin{aligned}
&\lambda + \frac{2(r_1 - s_1)}{\epsilon^2} - 2\delta\zeta_r(y_1, z_1, r_1, s_1) \\
&+ g\left(I^{\varepsilon_2}(y_1, r_1), \frac{2(y_1 - z_1)}{\epsilon^2} - 2\delta\zeta_y(y_1, z_1, r_1, s_1)\right) \leq 0.
\end{aligned} \tag{5.12}$$

Similarly, since the mapping $(z, s) \mapsto \Psi(y_1, z, r_1, s)$ has a maximum at the point (z_1, s_1), $u^{\varepsilon_1} - w$ has a minimum at (z_1, s_1) where w is defined by

$$w(z, s) \equiv u^{\varepsilon_2}(y_1, r_1) - \lambda(r_1 + s) - \frac{1}{\epsilon^2}\left((y_1 - z)^2 + (r_1 - s)^2\right) + 2\delta\zeta(y_1, z, r_1, s). \tag{5.13}$$

Since u^{ε_1} is a viscosity solution,

$$w_s(z_1, s_1) + g\left(I^{\varepsilon_1}(z_1, s_1), w_z(z_1, s_1)\right) \geq 0;$$

that is,

$$\begin{aligned} -\lambda + \frac{2(r_1 - s_1)}{\epsilon^2} + 2\delta\zeta_s(y_1, z_1, r_1, s_1) \\ + g\left(I^{\varepsilon_1}(z_1, s_1), \frac{2(y_1 - z_1)}{\epsilon^2} + 2\delta\zeta_z(y_1, z_1, r_1, s_1)\right) \geq 0. \end{aligned} \tag{5.14}$$

Subtracting eq (5.14) from eq (5.12) yields

$$2\lambda \leq g\left(I^{\varepsilon_1}(z_1, s_1), \frac{2(y_1 - z_1)}{\epsilon^2} + 2\delta\zeta_z\right) - g\left(I^{\varepsilon_2}(y_1, r_1), \frac{2(y_1 - z_1)}{\epsilon^2} - 2\delta\zeta_y\right) + 2\delta(\zeta_r + \zeta_s), \tag{5.15}$$

which we can rewrite as

$$\begin{aligned} 2\lambda \leq \left[g\left(I^{\varepsilon_1}(z_1, s_1), \frac{2(y_1 - z_1)}{\epsilon^2} + 2\delta\zeta_z\right) - g\left(I^{\varepsilon_1}(y_1, r_1), \frac{2(y_1 - z_1)}{\epsilon^2} + 2\delta\zeta_z\right)\right] \\ + \left[g\left(I^{\varepsilon_1}(y_1, r_1), \frac{2(y_1 - z_1)}{\epsilon^2} + 2\delta\zeta_z\right) - g\left(I^{\varepsilon_2}(y_1, r_1), \frac{2(y_1 - z_1)}{\epsilon^2} + 2\delta\zeta_z\right)\right] \\ + \left[g\left(I^{\varepsilon_2}(y_1, r_1), \frac{2(y_1 - z_1)}{\epsilon^2} + 2\delta\zeta_z\right) - g\left(I^{\varepsilon_2}(y_1, r_1), \frac{2(y_1 - z_1)}{\epsilon^2} - 2\delta\zeta_y\right)\right] + 2\delta(\zeta_r + \zeta_s). \end{aligned} \tag{5.16}$$

From property 5.1 we know that g is locally Lipschitz with respect to u_y,

$$|g\left(I(x), p\right) - g\left(I(x), q\right)| \leq C|p - q|. \tag{5.17}$$

From property 4.1 and property 5.2, we know that g is locally Lipschitz with respect to x,

$$|g\left(I^{\varepsilon_i}(x), p\right) - g\left(I^{\varepsilon_i}(\xi), p\right)| \leq C|x - \xi|, \tag{5.18}$$

where the Lipschitz constant C depends on i. Finally from property 4.2 of I and property 5.2 of $g(I, u_y)$ we have the crucial property

$$g\left(I^{\varepsilon_1}(x), p\right) < g\left(I^{\varepsilon_2}(x), p\right). \tag{5.19}$$

Therefore, from eq (5.16) we have for some constant C

$$\lambda \leq C\left(\delta + \sqrt{(y_1 - z_1)^2 + (r_1 - s_1)^2}\right). \tag{5.20}$$

However, since $\Psi(y_1, z_1, r_1, s_1) \geq \Psi(y_1, y_1, r_1, r_1)$, we see that

$$u^{\varepsilon_2}(y_1, r_1) - u^{\varepsilon_1}(z_1, s_1) - \lambda(r_1 + s_1) - \frac{1}{\epsilon^2}\left((y_1 - z_1)^2 + (r_1 - s_1)^2\right) + 2\delta\zeta(y_1, z_1, r_1, s_1)$$

$$\geq u^{\varepsilon_2}(y_1, r_1) - u^{\varepsilon_1}(y_1, r_1) - 2\lambda r_1 + 2\delta\zeta(y_1, y_1, r_1, r_1). \tag{5.21}$$

Consequently,

$$\begin{aligned} &\frac{1}{\epsilon^2}\left((y_1 - z_1)^2 + (r_1 - s_1)^2\right) \\ &\leq u^{\varepsilon_1}(y_1, r_1) - u^{\varepsilon_1}(z_1, s_1) + \lambda(r_1 - s_1) + 2\delta\left(\zeta(y_1, z_1, r_1, s_1) - \zeta(y_1, y_1, r_1, r_1)\right), \end{aligned} \tag{5.22}$$

which implies that $\sqrt{(y_1 - z_1)^2 + (r_1 - s_1)^2} = O(\epsilon)$ as $\epsilon \to 0$. Therefore, as we let ϵ and δ approach zero, we obtain from eq (5.20) the contradiction

$$\lambda \leq 0. \qquad \blacksquare \tag{5.23}$$

Remark: The proof in Theorem 5.1 also establishes that if u_1 is the solution to $u_r + g(I_1, u_y) = 0$ and u_2 is the solution to $u_r + g(I_2, u_y) = 0$, then $I_1 \geq I_2 \Rightarrow u_1 \geq u_2 \; \forall (y, r) \in \overline{\Omega}$. Further, this extends to any other function $\hat{g}(I, u_y)$ as long as $\hat{g}(I_1, u_y)$ and $\hat{g}(I_2, u_y)$ satisfy the four hypotheses of Theorem A and $\frac{\partial \hat{g}}{\partial I} < 0$.

From Theorem 5.1 we have that the $u^\varepsilon(y, r)$ decrease monotonically as $\varepsilon \to 0$, therefore the pointwise limit of $u^\varepsilon(y, r)$ must exist as $\varepsilon \to 0$. We can now define the *upper solution*, $\bar{u}$, as this limit:

$$\bar{u}(y, r) \equiv \lim_{\varepsilon \to 0} u^\varepsilon(y, r). \tag{5.24}$$

The lower solution is defined by an analogous process: Instead of defining the intensity function at points of discontinuity using the upper limit as in eq (4.1), suppose that instead we use the lower limit, i.e., $I(x) = \liminf_{\xi \to x} I(\xi)$. The approximate intensity functions are then defined, in contrast to eq (4.2), as

$$I_\varepsilon(x) = \inf_\xi \left(I(\xi) + \frac{1}{\varepsilon}|x - \xi|\right). \tag{5.25}$$

These approximate intensities retain properties 4.1 and 4.3 while property 4.2 merely takes the opposite monotonicity, i.e.,
Property 4.1(a): $I_\varepsilon(x)$ is Lipschitz continuous with Lipschitz constant $\frac{1}{\varepsilon}$.
Property 4.2(a): $\varepsilon_1 \geq \varepsilon_2 \Rightarrow I_{\varepsilon_1}(x) \leq I_{\varepsilon_2}(x) \; \forall x$.
Property 4.3(a): $\lim_{\varepsilon \to 0} I_\varepsilon(x) = I(x)$.
Because of property 4.2(a), Theorem 5.1 now implies that u_ε, the approximate solutions corresponding to these approximate intensities, must be nondecreasing as $\varepsilon \to 0$. Therefore we can define the *lower solution*, $\underline{u}$, as the limit of these monotonically increasing approximate solutions:

$$\underline{u}(y, r) \equiv \lim_{\varepsilon \to 0} u_\varepsilon(y, r). \tag{5.26}$$

Since for any $\varepsilon > 0$, $I^\varepsilon(y, r) \geq I_\varepsilon(y, r)$, it follows from the remark above that $u^\varepsilon(y, r) \geq u_\varepsilon(y, r)$, which implies $\bar{u}(y, r) \geq \underline{u}(y, r)$. When it can be established that $\bar{u}(y, r) \leq \underline{u}(y, r)$, we have that $\bar{u}(y, r) = \underline{u}(y, r)$, and we can define the solution, $u(y, r)$, as this common limit:

$$u(y, r) \equiv \bar{u}(y, r) = \underline{u}(y, r). \tag{5.27}$$

While the inequality $\bar{u}(y,r) \leq \underline{u}(y,r)$ generally appears to hold (see section 6), further work is needed to rigorously establish that this is the case. A partial answer, however, is provided by the following theorem, which we will use to rigorously establish that the solution in (5.27) is defined for a large class of discontinuous intensity functions. Theorem 5.2 shows that the difference between u^ε and u_ε on $\bar{\Omega}$ is bounded by the difference between u^ε and u_ε on the set D_ε, which we define by

$$D_\varepsilon \equiv \{(y,r) \in \Omega' | I^\varepsilon(y,r) \neq I_\varepsilon(y,r)\}. \tag{5.28}$$

We note that in general for small ε, D_ε is a set of points within $O(\varepsilon)$ distance from the discontinuities in the intensity function, $I(y,r)$.

Theorem 5.2: $\forall \varepsilon > 0$, $\sup_{(y,r)\in D_\varepsilon} |u^\varepsilon - u_\varepsilon| = \sup_{(y,r)\in \bar{\Omega}} |u^\varepsilon - u_\varepsilon|$.

Proof: Assume the theorem is false. We know from Theorem 5.1 that $u^\varepsilon \geq u_\varepsilon$. Since $u^\varepsilon \not\equiv u_\varepsilon$ (as $u^\varepsilon \equiv u_\varepsilon$ would imply the theorem is true), we can define

$$\sup_{(y,r)\in\bar{\Omega}} (u^\varepsilon - u_\varepsilon) = \alpha > 0, \tag{5.29}$$

and we can also define

$$\sup_{(y,r)\in\bar{\Omega}} (u^\varepsilon - u_\varepsilon) - \sup_{(y,r)\in D_\varepsilon} (u^\varepsilon - u_\varepsilon) = \gamma > 0. \tag{5.30}$$

Choose $\epsilon > 0$, $0 < \lambda < \frac{\gamma}{8(R_2 - R_1)}$, and define

$$\Phi(y,z,r,s) \equiv u^\varepsilon(y,r) - u_\varepsilon(z,s) - \lambda(r+s) - \frac{1}{\epsilon^2}\left((y-z)^2 + (r-s)^2\right), \tag{5.31}$$

where $y, z \in (-\infty, \infty)$ and $r, s \geq R_1$. Now choose $0 < \delta < \gamma/4$ and select a point $(y_0, z_0, r_0, s_0) \in (-\infty,\infty)^2 \times [R_1, R_2]^2$ with

$$\Phi(y_0, z_0, r_0, s_0) \geq \sup_{\bar{\Omega}\times\bar{\Omega}} \Phi(y,z,r,s) - \delta. \tag{5.32}$$

As in the proof of Theorem 5.1, we (1) define C_ε and C^ε to be the Lipschitz constants of u_ε and u^ε respectively; i. e.,

$$|u_\varepsilon(y,r) - u_\varepsilon(z,s)| \leq C_\varepsilon \sqrt{(y-z)^2 + (r-s)^2} \tag{5.33a}$$

$$|u^\varepsilon(y,r) - u^\varepsilon(z,s)| \leq C^\varepsilon \sqrt{(y-z)^2 + (r-s)^2} \tag{5.33b}$$

where $y, z \in (-\infty,\infty)$, $r, s \in [R_1, R_2]$, (2) use this Lipschitz continuity to show that for sufficiently small ϵ, there exists a $\mu > 0$ such that $(r_0 - R_1) \geq \mu > 0$ and $(s_0 - R_1) \geq \mu > 0$, (3) define

$$\Psi(y,z,r,s) \equiv \Phi(y,z,r,s) + 2\delta\zeta(y,z,r,s), \tag{5.34}$$

where $\zeta(y,z,r,s)$ is a smooth cutoff function with the properties $\zeta \in [0,1]$, $\zeta(y_0,z_0,r_0,s_0) = 1$, and $\zeta(y,z,r,s) = 0$ if $(y-y_0)^2+(z-z_0)^2+(r-r_0)^2+(s-s_0)^2 > \mu^2/4$, and (4) establish that the maximum of Ψ is attained at a point, (y_1,z_1,r_1,s_1), that is inside the support of ζ and therefore $r_1, s_1 > \mu/2 + R_1$.

We next work towards establishing that $(y_1,r_1) \notin D_\varepsilon$. We begin by considering any point (x,t) satisfying

$$u^\varepsilon(x,t) - u_\varepsilon(x,t) \geq \alpha - \frac{\gamma}{4}. \tag{5.35}$$

By the definition of α and γ in (5.29) and (5.30), we see that $(x,t) \notin D_\varepsilon$. From (5.31) and (5.35) we have that

$$\Phi(x,x,t,t) \geq \alpha - \gamma/4 - 2\lambda R_2. \tag{5.36}$$

We now work to determine a lower bound on $\Phi(x,x,t,t) - \Phi(Y,z,R,s)$ for $(Y,R) \in D_\varepsilon$. From (5.31) we have that

$$\Phi(Y,z,R,s) = [u^\varepsilon(Y,R) - u_\varepsilon(Y,R)] + [u_\varepsilon(Y,R) - u_\varepsilon(z,s)] - \lambda(R+s) - \frac{1}{\epsilon^2}\left((Y-z)^2+(R-s)^2\right). \tag{5.37}$$

From (5.29) and (5.30), we have that $[u^\varepsilon(Y,R) - u_\varepsilon(Y,R)] \leq \alpha - \gamma$, therefore

$$\Phi(Y,z,R,s) \leq \alpha - \gamma + [u_\varepsilon(Y,R) - u_\varepsilon(z,s)] - 2\lambda R_1 - \frac{1}{\epsilon^2}\left((Y-z)^2+(R-s)^2\right). \tag{5.38}$$

Combining this result with (5.36) and the fact that $\lambda < \frac{\gamma}{8(R_2-R_1)}$, we obtain the desired lower bound:

$$\Phi(x,x,t,t) - \Phi(Y,z,R,s) \geq \frac{\gamma}{2} - [u_\varepsilon(Y,R) - u_\varepsilon(z,s)] + \frac{1}{\epsilon^2}\left((Y-z)^2+(R-s)^2\right). \tag{5.39}$$

Using contradiction, we will now establish that for sufficiently small ϵ, we have that

$$\Phi(x,x,t,t) - \Phi(Y,z,R,s) > \frac{\gamma}{4}. \tag{5.40}$$

If (5.40) were false, then (5.39) implies that

$$\frac{1}{\epsilon^2}\left((Y-z)^2+(R-s)^2\right) \leq \frac{\gamma}{4} - \frac{\gamma}{2} + [u_\varepsilon(Y,R) - u_\varepsilon(z,s)]; \tag{5.41}$$

therefore, since u_ε is bounded, $\sqrt{(Y-z)^2+(R-s)^2} = O(\epsilon)$. By (5.33a),

$$|u_\varepsilon(Y,R) - u_\varepsilon(z,s)| \leq C_\varepsilon\sqrt{(Y-z)^2+(R-s)^2}.$$

Therefore, if $\epsilon > 0$ is chosen to be small enough that $C_\varepsilon\sqrt{(Y-z)^2+(R-s)^2} < \frac{\gamma}{4}$, we have from (5.39) that

$$\Phi(x,x,t,t) - \Phi(Y,z,R,s) > \frac{\gamma}{2} - \frac{\gamma}{4} = \frac{\gamma}{4}, \tag{5.42}$$

which contradicts the assumption that (5.40) is false, therefore (5.40) must be true.

With (5.40) in place, we can now show that $(y_1, r_1) \notin D_\varepsilon$. From (5.32) and (5.34), we see that

$$\Psi(y_1, z_1, r_1, s_1) \geq \Phi(y_0, z_0, r_0, s_0) + 2\delta \geq \sup_{\bar{\Omega}\times\bar{\Omega}} \Phi(y, z, r, s) + \delta \geq \Phi(x, x, t, t) + \delta. \tag{5.43}$$

Applying (5.40) to (5.43), we have for any $(Y, R) \in D_\varepsilon$,

$$\Psi(y_1, z_1, r_1, s_1) > \Phi(Y, z, R, s) + \frac{\gamma}{4} + \delta = \Phi(Y, z, R, s) + \frac{\gamma}{4} + 2\delta - \delta \geq \Psi(Y, z, R, s) + \frac{\gamma}{4} - \delta. \tag{5.44}$$

Since $\delta < \frac{\gamma}{4}$, we see that $\Psi(y_1, z_1, r_1, s_1) > \Psi(Y, z, R, s)$, and so, by setting $z = z_1$ and $s = s_1$, we conclude that $(y_1, r_1) \notin D_\varepsilon$.

Using the argument presented in (5.11)–(5.15) for Theorem 5.1, we obtain the following analog of (5.15):

$$2\lambda \leq g\left(I_\varepsilon(z_1, s_1), \frac{2(y_1 - z_1)}{\epsilon^2} + 2\delta\zeta_z\right) - g\left(I^\varepsilon(y_1, r_1), \frac{2(y_1 - z_1)}{\epsilon^2} - 2\delta\zeta_y\right) + 2\delta(\zeta_r + \zeta_s), \tag{5.45}$$

which we rewrite as

$$\begin{aligned} 2\lambda \leq & \left[g\left(I_\varepsilon(z_1, s_1), \frac{2(y_1 - z_1)}{\epsilon^2} + 2\delta\zeta_z\right) - g\left(I_\varepsilon(y_1, r_1), \frac{2(y_1 - z_1)}{\epsilon^2} + 2\delta\zeta_z\right)\right] \\ & + \left[g\left(I_\varepsilon(y_1, r_1), \frac{2(y_1 - z_1)}{\epsilon^2} + 2\delta\zeta_z\right) - g\left(I^\varepsilon(y_1, r_1), \frac{2(y_1 - z_1)}{\epsilon^2} + 2\delta\zeta_z\right)\right] \\ & + \left[g\left(I^\varepsilon(y_1, r_1), \frac{2(y_1 - z_1)}{\epsilon^2} + 2\delta\zeta_z\right) - g\left(I^\varepsilon(y_1, r_1), \frac{2(y_1 - z_1)}{\epsilon^2} - 2\delta\zeta_y\right)\right] + 2\delta(\zeta_r + \zeta_s). \end{aligned} \tag{5.46}$$

From property 5.1 we know that g is locally Lipschitz with respect to u_y, specifically,

$$|g\left(I^\varepsilon(x), p\right) - g\left(I^\varepsilon(x), q\right)| \leq C|p - q|. \tag{5.47}$$

From property 4.1 and property 5.2, we know that g is locally Lipschitz with respect to x, specifically

$$|g\left(I_\varepsilon(x), p\right) - g\left(I_\varepsilon(\xi), p\right)| \leq C|x - \xi|, \tag{5.48}$$

where the Lipschitz constant C depends on ε. Finally, by the definition of D_ε, we have for all $x \notin D_\varepsilon$,

$$g\left(I_\varepsilon(x), p\right) = g\left(I^\varepsilon(x), p\right). \tag{5.49}$$

Therefore, from eq (5.46) and the crucial fact that $(y_1, r_1) \notin D_\varepsilon$, we have for some constant C

$$\lambda \leq C\left(\delta + \sqrt{(y_1 - z_1)^2 + (r_1 - s_1)^2}\right). \tag{5.50}$$

However, since $\Psi(y_1, z_1, r_1, s_1) \geq \Psi(y_1, y_1, r_1, r_1)$, we see that

$$u^\varepsilon(y_1, r_1) - u_\varepsilon(z_1, s_1) - \lambda(r_1 + s_1) - \frac{1}{\epsilon^2}\left((y_1 - z_1)^2 + (r_1 - s_1)^2\right) + 2\delta\zeta(y_1, z_1, r_1, s_1)$$

$$\geq u^\varepsilon(y_1, r_1) - u_\varepsilon(y_1, r_1) - 2\lambda r_1 + 2\delta\zeta(y_1, y_1, r_1, r_1). \tag{5.51}$$

Consequently,

$$\frac{1}{\epsilon^2}\left((y_1 - z_1)^2 + (r_1 - s_1)^2\right)$$

$$\leq u_\varepsilon(y_1, r_1) - u_\varepsilon(z_1, s_1) + \lambda(r_1 - s_1) + 2\delta\left(\zeta(y_1, z_1, r_1, s_1) - \zeta(y_1, y_1, r_1, r_1)\right), \tag{5.52}$$

which implies that $\sqrt{(y_1 - z_1)^2 + (r_1 - s_1)^2} = O(\epsilon)$ as $\epsilon \to 0$. Therefore, as we let ϵ and δ approach zero, we obtain from (5.50) the contradiction

$$\lambda \leq 0. \qquad \blacksquare \tag{5.53}$$

Remark: The proof of the theorem also extends to any function $\hat{g}(I, u_y)$ where $\hat{g}(I_1, u_y)$ and $\hat{g}(I_2, u_y)$ satisfy the four hypotheses of Theorem A; specifically, if u_1 is the solution to $u_r + \hat{g}(I_1, u_y) = 0$, u_2 is the solution to $u_r + \hat{g}(I_2, u_y) = 0$, D is the set $\{(y, r) \in \Omega' | I_1 \neq I_2\}$, and we require that $u_1(y, 0) \equiv u_2(y, 0)$, then $\sup_{(y,r)\in D} |u_1 - u_2| = \sup_{(y,r)\in\bar{\Omega}} |u_1 - u_2|$.

We now explore some cases where, if we assume the Lipschitz constants of u^ε and u_ε are independent of ε, Theorem 5.2 guarantees that the upper solution and the lower solution coincide, and therefore the solution is defined. (The assumption that u^ε and u_ε are equilipschitz is unlikely to be violated since I (and therefore I^ε and I_ε) is bounded away from 0 and ∞; it follows that violations of the equilipschitz assumption would require unusual behavior such as a sequence of $(y_\varepsilon, r_\varepsilon)$ where, as $\varepsilon \to 0$, $u^\varepsilon_r \to \infty$ and $C_1(u^\varepsilon_r)^2 \leq u^\varepsilon_y \leq C_2(u^\varepsilon_r)^2$ for some constants C_1 and C_2 (or $u_{\varepsilon,r} \to \infty$ and $C_1(u_{\varepsilon,r})^2 \leq u_{\varepsilon,y} \leq C_2(u_{\varepsilon,r})^2$) or an infinite number of gradient discontinuities converge as $\varepsilon \to 0$ to a point inducing Cantor function-like behavior.)

For any characteristic curve, $Y(r)$, describing the propagation of information in (5.1), we have that $Y'(r) = \frac{\partial g}{\partial u_y}$. Since $\left|\frac{\partial g}{\partial u_y}\right| < \frac{1}{2}$ (from property 5.1), the maximum speed of the characteristics is $\frac{1}{2}$.

Now consider an intensity I defined on Ω that is discontinuous only on a Lipschitz curve $C(y)$ with Lipschitz constant ≤ 2. If we use J to denote the bound on the magnitude of $I(y, r)$, then the region D_ε (defined in (5.28)) must be contained within E_ε, the region bounded by $y = Y_0$, $y = Y_1$, the curve L — which we define as all points lying below C that are distance $J\varepsilon$ from C — and the curve B — which we define as all points lying above C that are distance $J\varepsilon$ from C (see fig. 3). The fact that $C(y)$ has Lipschitz constant ≤ 2 implies that $L(y)$ must also be Lipschitz continuous with Lipschitz constant ≤ 2, therefore the characteristic curves cannot exit E_ε through L. Since information only propagates *into*

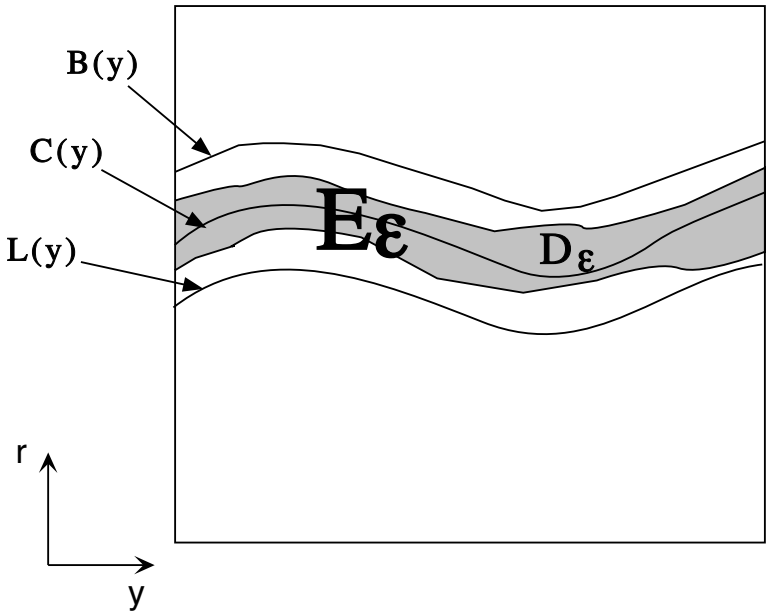

Figure 3: *Region near the discontinuity. $C(y)$ is a curve where I is discontinuous, which induces the region D_ε, where I^ε differs from I_ε. From Theorem 5.2, we know that the maximum value of $|u^\varepsilon - u_\varepsilon|$ is attained in D_ε. D_ε is contained within the region E_ε, which is bounded by $B(y)$ and $L(y)$.*

E_ε through L and $I^\varepsilon = I_\varepsilon$ for all points below L (as D_ε lies strictly above L), we must have that $u^\varepsilon = u_\varepsilon$ on L. Since E_ε is a strip that is only $2J\varepsilon$ thick, we have that

$$|u^\varepsilon(y,r) - u_\varepsilon(y,r)| \leq 4MJ\varepsilon \qquad \forall (y,r) \in E_\varepsilon, \tag{5.54}$$

where M denotes the common Lipschitz constant for all u^ε and u_ε. Since $D_\varepsilon \subset E_\varepsilon$, we have from (5.54) that $\lim_{\varepsilon \to 0} \sup_{(y,r)\in D_\varepsilon} |u^\varepsilon - u_\varepsilon| = 0$ uniformly over D_ε. Applying Theorem 5.2, we have that

$$\lim_{\varepsilon \to 0} \sup_{(y,r)\in \bar{\Omega}} |u^\varepsilon - u_\varepsilon| = \lim_{\varepsilon \to 0} \sup_{(y,r)\in D_\varepsilon} |u^\varepsilon - u_\varepsilon| = 0. \tag{5.55}$$

Therefore $\bar{u} = \underline{u}$ and the solution is defined. (We also note that this argument can easily be extended to establish that the solution is defined when the intensity function has multiple (but finite) curves of discontinuity in the intensity — as long as each curve is Lipschitz continuous with Lipschitz constant ≤ 2.)

We now consider three examples where the intensity functions and boundary conditions correspond to two intersecting planes.

For our first example, we consider the solution for the intensity and boundary conditions from the intersection of the plane $u = y + r$ on the left with the plane $u = \frac{3}{4}r$ on the

right (therefore the line of the intersection/intensity discontinuity is $y = -\frac{1}{4}r$). The speed, $Y'(r)$, of the characteristics to the left of the intersection is $-\frac{1}{5}$, so, since the characteristics propagate with increasing r *into* the line of discontinuity, we still have that $u^\varepsilon = u_\varepsilon$ on the curve L (even though the magnitude of the slope of the line of discontinuity equals 4 here, which is greater than the bound of 2 used before). Since $u^\varepsilon = u_\varepsilon$ on L, we can apply Theorem 5.2 to guarantee that $\bar{u} = \underline{u}$ (i.e., the solution exists). Since the solution exists, the methods of the next section can be used to verify that this solution does indeed correspond to the original two planes and so the characteristics to the right of the intersection have speed 0.

We can use this example to demonstrate that our notion of the solution as a common limit allows the solution to be defined for cases where the previous notion of solution for Hamilton-Jacobi equations with discontinuous spatial dependence — given by Ishii in [9] — fails to apply. Ishii expanded Crandall and Lion's definition of viscosity solution to some cases with discontinuous spatial dependence using the following definition:

Definition (Ishii viscosity solution): A function $u \in C(\overline{\Omega})$ is an *Ishii viscosity solution* of an equation of the form $u_r(x) + H(x, u_y(x)) = 0$ if for any (smooth) function $\phi \in C^1(\Omega')$, we have that

(a) At any point $x_0 \in \Omega'$ where $u(x) - \phi(x)$ attains a local maximum, we have that $\phi_r(x_0) + \limsup_{x \to x_0} H(x, \phi_y(x_0)) \leq 0$,

and

(b) At any point $x_0 \in \Omega'$ where $u(x) - \phi(x)$ attains a local minimum, we have that $\phi_r(x_0) + \liminf_{x \to x_0} H(x, \phi_y(x_0)) \geq 0$.

We now show that our two plane solution, u, is not an Ishii viscosity solution: Select $\phi = y + r - [(y - y_0)^2 + (r - r_0)^2]$ where (y_0, r_0) is some point on the line of discontinuity. $u - \phi$ has a maximum at (y_0, r_0) and $\phi_y(y_0, r_0) = \phi_r(y_0, r_0) = 1$, therefore, if the Ishii viscosity solution is defined, we have that

$$1 + \limsup_{x \to (y_0, r_0)} g(I(x), 1) \leq 0. \tag{7.4}$$

To the left of the discontinuity, we have that $I = \frac{1}{\sqrt{3}}$, to the right of the discontinuity, we have that $I = \frac{9}{20}$ $\left(< \frac{1}{\sqrt{3}}\right)$. Since $u = y + r$ to the left of the discontinuity, we know that $1 + g\left(\frac{1}{\sqrt{3}}, 1\right) = 0$, therefore, since $\frac{\partial g}{\partial I} < 0$ (property 5.2),

$$0 = 1 + g\left(\frac{1}{\sqrt{3}}, 1\right) < 1 + g\left(\frac{9}{20}, 1\right) = 1 + \limsup_{x \to (y_0, r_0)} g(I(x), 1). \tag{7.5}$$

From the contradiction of (7.5) with (7.4), we have that the solution is not an Ishii viscosity solution.

Our second planar example demonstrates that our notion of solution also differs from the notion of an entropy solution. In entropy solutions, characteristics cannot originate and propagate *out* from a curve of discontinuity. For this example, we use the intensity

and boundary conditions corresponding to $u = y + \frac{4}{3}r$ to the left of the discontinuity and $u = \frac{43}{39}r$ to the right of the discontinuity. Since the line of discontinuity is $y = -\frac{3}{13}r$ and the characteristic speed is $-\frac{3}{13}$ to the left of the discontinuity, L is a line parallel to the line of discontinuity, and we again have that $u^\varepsilon = u_\varepsilon$ on L; therefore Theorem 5.2 guarantees that $\bar{u} = \underline{u}$ and the solution is defined. Again the methods of the next section verify that this solution corresponds to the two original planes. Since the characteristics corresponding to the plane to the right of the discontinuity have speed 0, we see that characteristics originate and emanate upward from the discontinuity, therefore, our solution is clearly not an entropy solution. We note that it is not uncommon for discontinuous spatial data to lead to non-entropy solutions (for example, see Lyons [15]); here, in contrast with continuous intensity cases, we see that the unique solution of interest can be one of these non-entropy solutions.

Our third example is a case where Theorem 5.2 cannot be used to guarantee that $\bar{u} = \underline{u}$. In this example, to the left of the discontinuity, $u = y + \frac{6}{5}r$ and the characteristic speed is $-\frac{15}{68} \doteq -\frac{1}{4.53}$ and, to the right of the discontinuity, $u = r$ and the characteristic speed is 0. Since the line of discontinuity is $y = -\frac{1}{5}r$, characteristics emanate out from both sides of the discontinuity. Since characteristics may pass through D_ε before reaching L or B, we cannot guarantee that $u^\varepsilon = u_\varepsilon$ on either L or B, therefore Theorem 5.2 cannot be exploited to establish that $\bar{u} = \underline{u}$. Despite the fact that we have not rigorously established that $\bar{u} = \underline{u}$, we will present numerical evidence in the next section which indicates that $\bar{u} = \underline{u}$ is likely to be true (and therefore the solution is defined).

6 Convergence of Monotonic Numerical Schemes

In this section, we show that if $u(y, r)$ is defined (using the definition from section 5) and the approximate solutions $u^\varepsilon(y, r)$ and $u_\varepsilon(y, r)$ are equilipschitz, then monotone finite difference schemes must converge to $u(y, r)$ as their mesh size decreases.

We begin by introducing notation for the numerical solution. Given mesh sizes $\Delta y, \Delta r > 0$, we will use U_j^n to denote the numerical approximation to $u(j\Delta y, n\Delta r)$, the solution at the grid points where $j \in \mathbf{Z}, n \in \mathbf{Z}^+$. Also I_j^n will be used as an abbreviation for $I(j\Delta y, n\Delta r)$. Our (explicit) numerical scheme marches forward in r by the formula

$$U_j^{n+1} = F\left(I_j^n, U_{j-p}^n, U_{j-p+1}^n, ..., U_{j+q}^n\right), \tag{6.1}$$

where F can be expressed as the following, which more clearly parallels the Hamilton-Jacobi equation form:

$$F\left(I_j^n, U_{j-p}^n, U_{j-p+1}^n, ..., U_{j+q}^n\right)$$
$$\equiv U_j^n - \Delta r f\left(I_j^n, \frac{\left(U_{j-p+1}^n - U_{j-p}^n\right)}{\Delta y},\right.$$

$$\frac{\left(U^n_{j-p+2} - U^n_{j-p+1}\right)}{\Delta y}, ..., \frac{\left(U^n_{j+q} - U^n_{j+q-1}\right)}{\Delta y}\right). \tag{6.2}$$

We require f to be *consistent* with eq (5.1), the SAR SFS equation, i.e.,

$$f(I, a, a, ...a) = g(I, a), \tag{6.3}$$

and we also require F to be *monotone* on $[-K, K]$; i.e., $F(I, a_1, a_2, ..., a_{p+q})$ is a nondecreasing function of each of the a_i when the absolute value of each of the numerical differences (i.e., all the arguments of f except the first argument) are bounded by K. (In other words K is an a priori bound on the "numerical derivatives".)

From consistency and the fact that $\frac{\partial g}{\partial I} < 0$ (property 5.2), we have that $f(I, a, a, ...a)$ must be a decreasing function of I. We will further require that the f in our scheme is a decreasing function of I when the other arguments of f are not identical. We define a scheme with this property as *intensity monotone*.

As with all numerical evolution schemes for hyperbolic differential equations, the dependence upon previous data of the value assigned at a given point must correspond to the differential equation's dependence upon previous data or instability will arise. In order to select a monotone, consistent scheme, this CFL (Courant, Friedrichs, and Lewy) condition must be satisfied; i.e.,

$$\frac{\Delta r}{\Delta y} \leq \left|\frac{\partial g}{\partial u_y}\right|. \tag{6.4}$$

From property 5,1, we have that $\left|\frac{\partial g}{\partial u_y}\right|$ is bounded by $\frac{1}{2}$ so the CFL condition is satisfied as long as our mesh obeys the restriction

$$\frac{\Delta r}{\Delta y} \leq \frac{1}{2}. \tag{6.5}$$

Our convergence proof for the case of discontinuous intensities will make use of a previous result due to Souganidis [11] that extends the work of Crandall and Lions in [12] to establish numerical convergence when the intensity and viscosity solution are Lipschitz continuous. Specifically, if $u(y, r)$ is bounded and Lipschitz continuous with Lipschitz constant C and $I(y, r)$ is Lipschitz continuous with Lipschitz constant L, then monotone, consistent numerical schemes must converge to the solution as the mesh size shrinks; specifically,

$$|u(Y, R) - U(Y, R)| \leq K(C, L)(\Delta r)^{\frac{1}{2}}, \tag{6.6}$$

where $U(Y, R)$ denotes the numerical approximation to $u(Y, R)$, the value of the viscosity solution at some point (Y, R). The value of K in (6.6) depends not only on C and L but also on the initial condition's Lipschitz constant and maximum absolute value. Since we will be considering a series of schemes that all have the same initial condition, we suppress this dependence in our notation.

We are now ready to present the main result of this section:

Theorem 6.1 *(convergence): Assume $u(y,r)$ is defined (as in section 5) and assume that the approximate solutions, $u^\varepsilon(y,r)$ and $u_\varepsilon(y,r)$, have a common Lipschitz constant, M. Then explicit numerical algorithms of the form in eq (6.1) and eq (6.2) that are consistent, monotone, and intensity monotone must converge to the solution as the mesh size decreases, even when the intensity function, $I(y,r)$, is discontinuous on a set of measure zero; i.e.,*

$$U(Y,R) \overset{\Delta r \to 0}{\longrightarrow} u(Y,R), \tag{6.7}$$

where $U(Y,R)$ denotes the numerical approximation to $u(Y,R)$, the solution at the point (Y,R).

Proof: I^ε, the intensity leading to the approximate solution u^ε, is Lipschitz continuous. We wish to exploit the fact that convergence is known when the intensity is Lipschitz, so we relate the actual solution to the approximate solution:

$$u(Y,R)-U(Y,R) = [u(Y,R)-u^\varepsilon(Y,R)]+[u^\varepsilon(Y,R)-U^\varepsilon(Y,R)]+[U^\varepsilon(Y,R)-U(Y,R)], \tag{6.8}$$

where $U^\varepsilon(Y,R)$ denotes the numerical approximation to $u^\varepsilon(Y,R)$. We consider each of the three bracketed terms in eq (6.8) separately:

1. Minimizing $[u(Y,R) - u^\varepsilon(Y,R)]$ is straightforward since u^ε converges pointwise to u. Therefore

$$\lim_{\varepsilon \to 0}[u(Y,R) - u^\varepsilon(Y,R)] = 0. \tag{6.9}$$

2. To minimize $[u^\varepsilon(Y,R) - U^\varepsilon(Y,R)]$, we first note from (6.6) that the absolute value of this quantity is bounded by $K\left(C(\varepsilon), L(\varepsilon)\right)(\Delta r)^{\frac{1}{2}}$ since, from section 5, we know that the u^ε are (equi-)bounded. Since K increases monotonically as C, the Lipschitz constant of the solution, increases, and since $C(\varepsilon) \leq M$, we have that $K\left(C(\varepsilon), L(\varepsilon)\right) \leq K\left(M, L(\varepsilon)\right)$. To bound the effect of ε on L we will need to make ε a function of the mesh size, Δr. From property 4.1 we know that the intensity function used to determine u^ε has a Lipschitz constant of $\frac{1}{\varepsilon}$; therefore,

$$|u^\varepsilon(Y,R) - U^\varepsilon(Y,R)| \leq K\left(M, \frac{1}{\varepsilon}\right)(\Delta r)^{\frac{1}{2}}. \tag{6.10}$$

We now define the function $\varepsilon(\Delta r)$ by

$$\varepsilon(\Delta r) = \inf\left\{\varepsilon | \hat{\varepsilon} \geq \varepsilon \Rightarrow K\left(M, \frac{1}{\hat{\varepsilon}}\right) \leq \frac{1}{(\Delta r)^{\frac{1}{4}}}\right\}. \tag{6.11}$$

(We will always write this function's dependence explicitly to differentiate the function $\varepsilon(\Delta r)$ from the variable ε.) Since K can only approach infinity as $\varepsilon \to 0$ (that is, as the Lipschitz constant of the intensity becomes infinite), we have that

$$\lim_{\Delta r \to 0} \varepsilon(\Delta r) = 0, \tag{6.12}$$

and, by the construction of $\varepsilon(\Delta r)$ in (6.11), we also have that

$$|u^{\varepsilon}(Y,R) - U^{\varepsilon}(Y,R)| \leq K\left(M, \frac{1}{\varepsilon(\Delta r)}\right)(\Delta r)^{\frac{1}{2}} \leq (\Delta r)^{\frac{1}{4}}. \tag{6.13}$$

3. Next we bound the behavior of $[U^{\varepsilon}(Y,R) - U(Y,R)]$. Consider two vectors, V and W, where each of the components of V are greater than or equal to the corresponding components of W, i.e., $V_i \geq W_i$ for $i \in \mathbf{Z}$. Now consider $F(I, V_{j-p}, V_{j-p+1}, ..., V_{j+q}) - F(J, W_{j-p}, W_{j-p+1}, ..., W_{j+q})$ where $I \geq J$. We can rewrite this expression as

$$\begin{aligned} &F(I, V_{j-p}, V_{j-p+1}, ..., V_{j+q}) - F(J, W_{j-p}, W_{j-p+1}, ..., W_{j+q}) = \\ &[F(I, V_{j-p}, V_{j-p+1}, ..., V_{j+q}) - F(I, W_{j-p}, W_{j-p+1}, ..., W_{j+q})] + \\ &[F(I, W_{j-p}, W_{j-p+1}, ..., W_{j+q}) - F(J, W_{j-p}, W_{j-p+1}, ..., W_{j+q})], \end{aligned} \tag{6.14}$$

and note that the first bracketed term is nonnegative because the scheme is monotonic and the second bracketed term is nonnegative because the scheme is intensity monotonic. Therefore,

$$F(I, V_{j-p}, V_{j-p+1}, ..., V_{j+q}) - F(J, W_{j-p}, W_{j-p+1}, ..., W_{j+q}) \geq 0. \tag{6.15}$$

The initial condition for both u and u^{ε} are identical, therefore, $U(j,0) = U^{\varepsilon}(j,0)$ for $j \in \mathbf{Z}$. Further, from property 4.2, we have, for any ε, j, and n, that $I^{\varepsilon}(j,n) \geq I(j,n)$. Therefore, applying a standard induction argument to (6.1) and (6.15), we obtain, for any ε, that

$$U^{\varepsilon}(Y,R) - U(Y,R) \geq 0. \tag{6.16}$$

Now we return to eq (6.8), replacing ε with the function $\varepsilon(\Delta r)$, and take the limit as $\Delta r \to 0$.

$$\begin{aligned} \lim_{\Delta r \to 0}(u(Y,R) - U(Y,R)) &= \lim_{\Delta r \to 0}[u(Y,R) - u^{\varepsilon(\Delta r)}(Y,R)] \\ + \lim_{\Delta r \to 0}[u^{\varepsilon(\Delta r)}(Y,R) - U^{\varepsilon(\Delta r)}(Y,R)] &+ \lim_{\Delta r \to 0}[U^{\varepsilon(\Delta r)}(Y,R) - U(Y,R)]. \end{aligned} \tag{6.17}$$

From (6.9) and (6.12), the first bracketed term goes to zero. From (6.10) and (6.13), we see that the second bracketed term also goes to zero. From (6.16) we see that the third bracketed term is nonnegative. Therefore

$$\lim_{\Delta r \to 0}(u(Y,R) - U(Y,R)) \geq 0. \tag{6.18}$$

If we repeat the above argument but replace u^{ε}, the approximate solutions that converges to the actual solution from above, with u_{ε}, the sequence of approximate solutions that converges to the solution from below, we obtain the opposite inequality

$$\lim_{\Delta r \to 0}(u(Y,R) - U(Y,R)) \leq 0, \tag{6.19}$$

which, when combined with (6.18), yields the desired conclusion:

$$\lim_{\Delta r \to 0} (u(Y,R) - U(Y,R)) = 0. \qquad \blacksquare \tag{6.20}$$

We now consider two examples of finite difference schemes converging to the solution of the discontinuous SAR radar equation. Since monotone schemes are, at best, first order accurate, we choose instead to employ a third order essentially non-oscillatory (ENO) scheme — adapted from the algorithm presented in [14] — for the examples presented here. While the presence of discontinuous intensity data implies that we cannot hope for better than first order global accuracy (and, in fact, we will present evidence that the global accuracy is of order $\frac{1}{2}$), we use the third order scheme since it more closely models the behavior of the solution away from discontinuities in the solution's gradient.

Previously, we have considered the domain of the intensity data and the solution to be infinite; specifically, $y \in (-\infty, \infty)$ and $r \in (R_1, R_2)$. Of course, the domain of y in real radar data and in finite difference simulations must be restricted to some finite interval, so we now consider the rectangular domain $\Omega = \{(y,r) | y \in (Y_1, Y_2), r \in (R_1, R_2)\}$. For this domain, in addition to boundary conditions being needed on the edge at $r = R_1$, we now also specify the value of u along the edges of Ω at $y = Y_1$ and $y = Y_2$ since information (i.e., characteristic curves) can enter into Ω through these edges.

For our first example, we consider the intensity function corresponding to the surface

$$u(y,r) = 100r - 70\left(\arctan\left|r - 5 - \sin\left(\frac{y}{3}\right)\right| - 1\right)$$

$$+15\left[\sin\left(-\frac{r}{2} + \frac{2}{5}y\right) + \sin\left(r - \frac{y}{1.7}\right) + \sin\left(\frac{r}{2.9} + y\right)\right].$$

The intensity function is discontinuous along the curve $r = 5 + \sin\left(\frac{y}{3}\right)$. Since the magnitude of the slope of this curve is at most $\frac{1}{3}$, which is less than 2, we know from Section 5 that the solution $u (= \bar{u} = \underline{u})$ is guaranteed to be defined, and, from Theorem 6.1, the numerical scheme must converge to this solution. We consider the domain $\Omega = \{(y,r) : y \in (0,20), r \in (0,10)\}$ and apply the grid $\Delta r = \frac{1}{4}$ and $\Delta y = \frac{1}{2}$, which easily satisfies the CFL condition $\frac{\Delta r}{\Delta y} \leq 2$. In fig. 4(a) we display the ENO simulation of the surface using the intensity function and boundary conditions; for comparison, in fig. 4(b), we display the actual surface.

If we wish to recover $Z(x,y)$, the representation of the surface in standard Cartesian coordinates, we must rotate each of the points $(y, r, u(y,r))$ using the matrix transformation

$$\begin{pmatrix} x \\ y \\ z \end{pmatrix} = \begin{pmatrix} 0 & \cos\left(\frac{\pi}{2} - \varphi\right) & \sin\left(\frac{\pi}{2} - \varphi\right) \\ 1 & 0 & 0 \\ 0 & -\sin\left(\frac{\pi}{2} - \varphi\right) & \cos\left(\frac{\pi}{2} - \varphi\right) \end{pmatrix} \begin{pmatrix} y \\ r \\ u \end{pmatrix}, \tag{7.3}$$

where φ is the angle of inclination of the satellite (see fig. 1). The Cartesian representation of the surface is given in fig. 5.

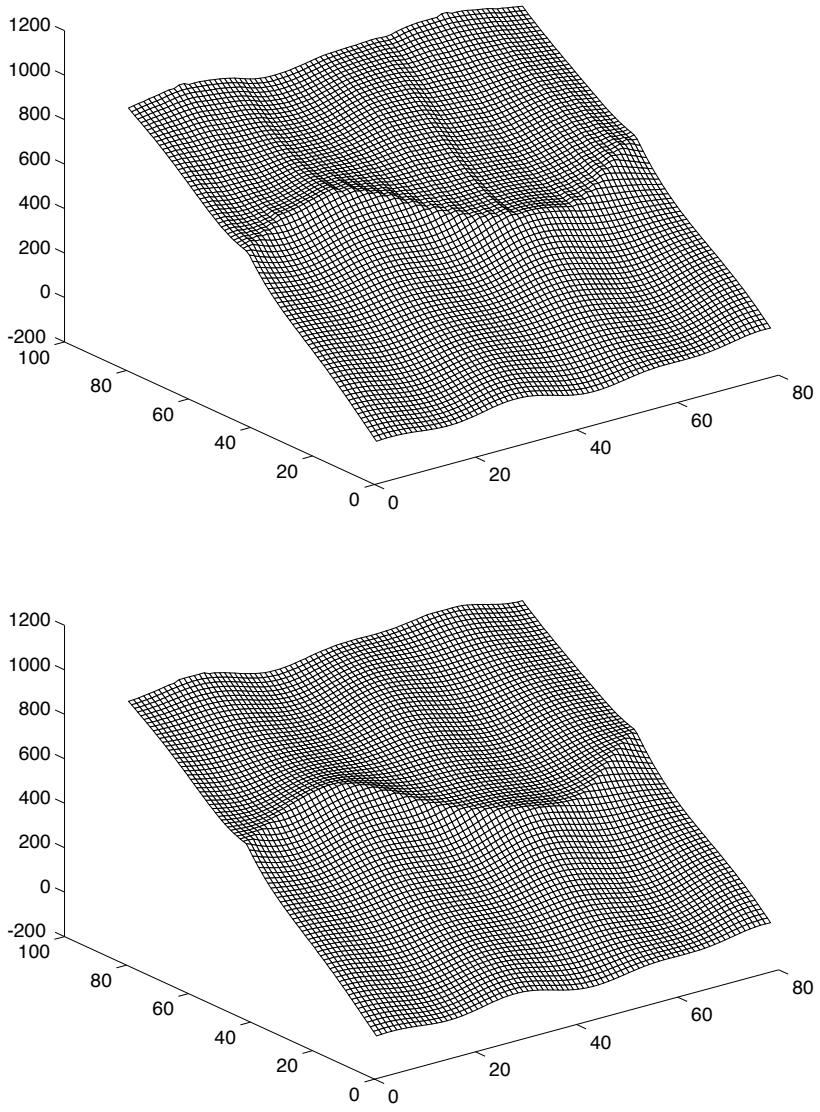

Figure 4: *Comparison of (a) numerical (top) and (b) actual (bottom) surfaces. The y pixel range displayed on the axis is [0,80]; the r pixel range displayed on the axis is* $[0, 100]$.

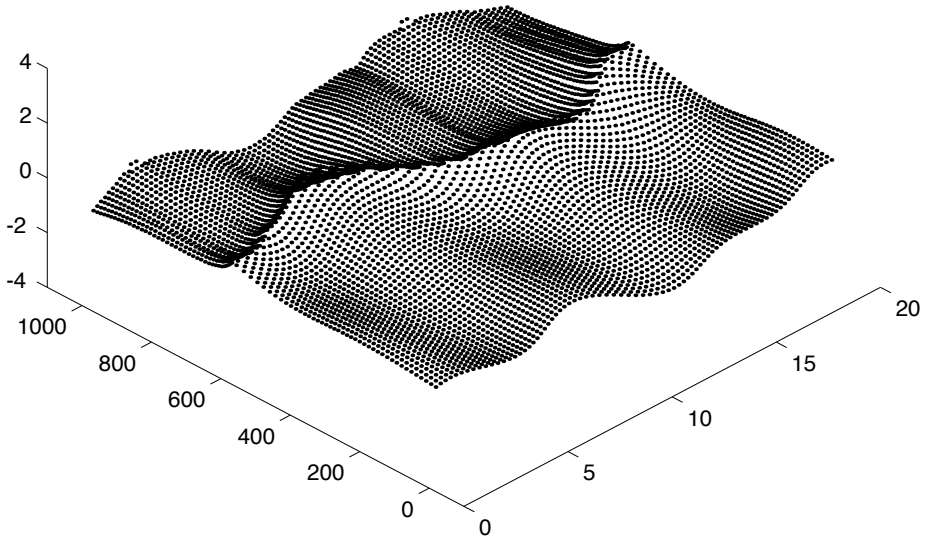

Figure 5: *Cartesian reconstruction of the surface in fig. 5. The y axis range is* $[0, 20]$*; the x axis range is* $[-50, 1050]$*. The ridged surface is now displayed as it would normally appear.*

For our final example, we return to the third planar example presented at the end of Section 5. For this case Theorem 5.2 could not be used to establish that $\bar{u} = \underline{u}$, therefore Theorem 6.1 cannot be applied. However, we present numerical evidence that $\bar{u} = \underline{u}$ and that this common limit corresponds to the original two planes. In fig. 6(a) we see that the L_1 norm at $r = 40$ (with $\Delta r = \Delta y = \frac{1}{2}$ and $y \in (-20, 20)$) of the difference between U^ε, the simulation of u^ε, and u, the two plane solution, converges to a small error as $\varepsilon \to 0$. fig. 6(b) exhibits the same behavior for U_ε, the simulation of u_ε. This error shrinks as the mesh size is decreased. In fig. 7, we simulate the solution using I (as opposed to I^ε or I_ε used for fig. 6) and monitor the L_1 norm of the difference between the numerical and the two plane solution at $r = 40$ as the numerical mesh, $\Delta r (= \Delta y)$, shrinks. The regression line shown in fig. 7, suggests that this L_1 error is approximately of order $\sqrt{\Delta r}$, which is the same as the theoretical bound on the error determined by Souganidis for monotone schemes applied to continuous intensities.

Acknowledgments: I would like to thank Paul Dupuis, Craig Evans, Stuart Geman, Donald McClure, and Chi-Wang Shu for helpful discussions and suggestions and also the two anonymous referees who made many helpful recommendations. I also wish to acknowledge the financial support of the National Science Foundation (Grant No. DMS-9704864) during the final stages of this work and the U.S. Army Research Office (Grant No. DAAL03-92-G-0115) and ARPA (Contract No. MDA972-93-1-0012) during some of the initial work.

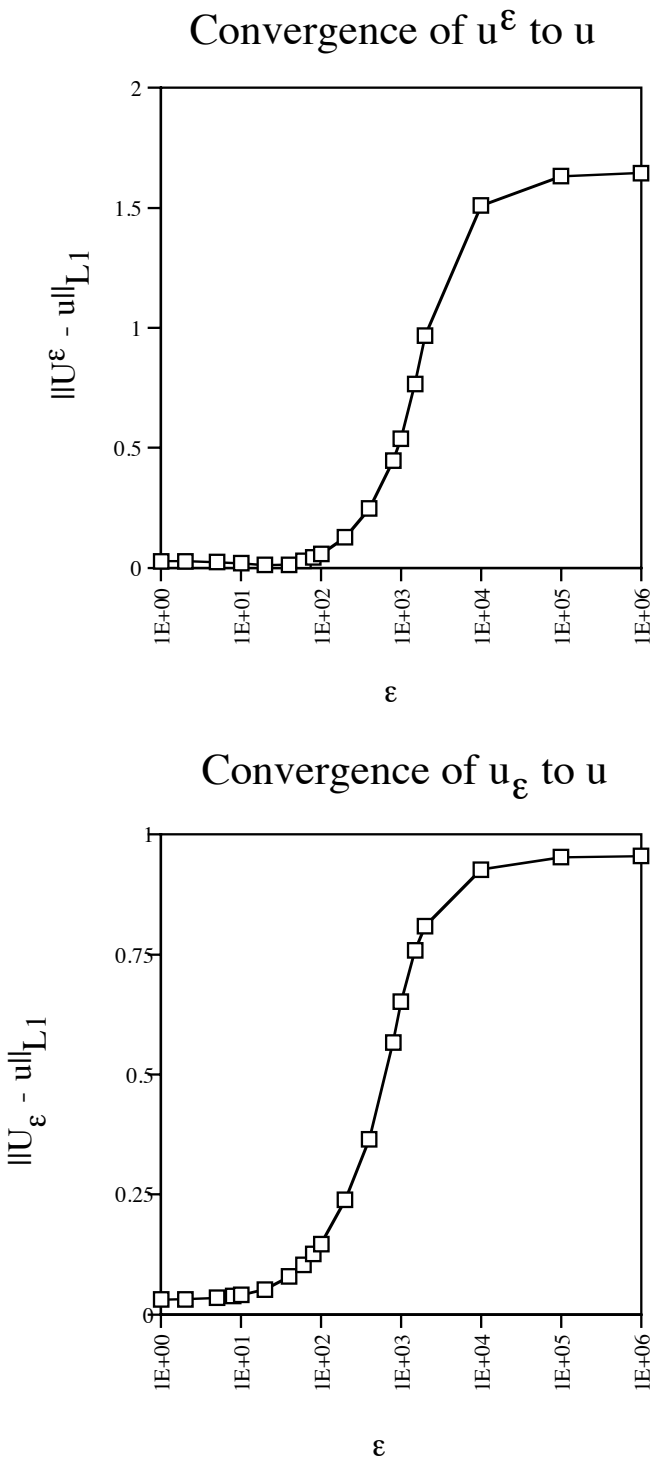

Figure 6: *Convergence of approximate solutions to the actual solution at* $r = 40$. *The displayed error accurately models the difference between the approximate solution and the two plane solution in the region* $\varepsilon \geq 60$, *where the numerical error is insignificant.*

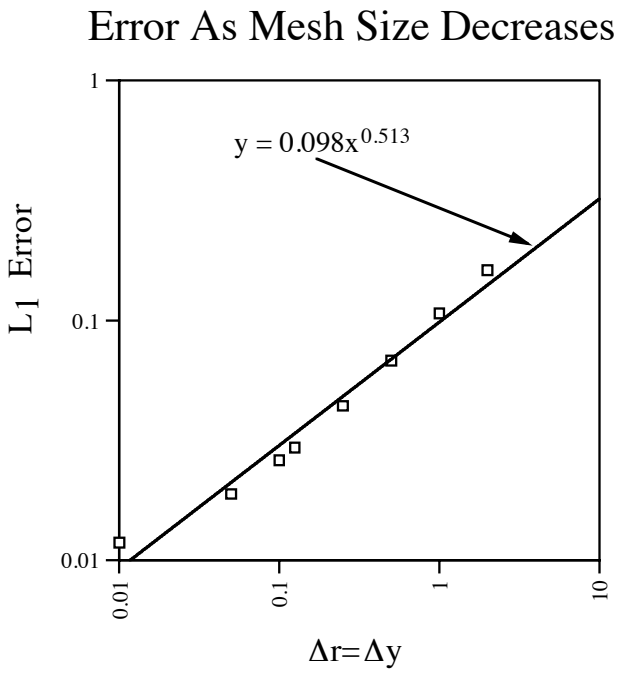

Figure 7: *Error between the numerical and actual solution at* $r = 40$ *as the mesh shrinks. The regression line for the data indicates an error of order* $(\Delta r)^{0.513}$*, which suggests that the theoretical error bound for monotone schemes applied to discontinuous data may be order* $(\Delta r)^{0.5}$*.*

References

[1] D. N. Ostrov, Boundary Conditions and Fast Algorithms for Surface Reconstructions from Synthetic Aperture Radar Data, to appear in *IEEE Transactions on Geoscience and Remote Sensing.*

[2] B. K. P. Horn, Obtaining Shapes from Shading Information, in *Psychology of Computer Vision*, McGraw-Hill, New York, 1975, pp. 115–155.

[3] P. Dupuis and J. Oliensis, An Optimal Control Formulation and Related Numerical Methods for a Problem in Shape Reconstruction, *Annals of Applied Probability*, Vol. **4**, 1993, pp. 287–345.

[4] E. Rouy and A. Tourin, A Viscosity Solutions Approach to Shape-From-Shading, *SIAM J. Numer. Anal.*, Vol. **29**, 1992, no. 3, pp. 867–884.

[5] M. G. Crandall and P. L. Lions, Viscosity Solutions of Hamilton-Jacobi Equations, *Trans. Amer. Math. Soc.*, Vol. **277**, 1983, pp. 1–42.

[6] M. G. Crandall, L. C. Evans, and P. L. Lions, Some Properties of Viscosity Solutions of Hamilton-Jacobi Equations, *Trans. Amer. Math. Soc.*, Vol. **282**, 1984, pp. 487–502.

[7] P. L. Lions, E. Rouy and A. Tourin, Shape-From-Shading, Viscosity Solutions, and Edges *Numer. Math.*, Vol. **64**, 1993, pp. 323–353.

[8] A. Tourin, A Comparison Theorem for a Piecewise Lipschitz Continuous Hamiltonian and Application to Shape-From-Shading Problems, *Numer. Math*, Vol. **62**, 1992, pp. 75–85.

[9] H. Ishii, Hamilton-Jacobi Equations with Discontinuous Hamiltonians on Arbitrary Open Subsets, *Bull. Fac. Sci. Engrg. Chuo Univ.*, Vol. **28**, 1985, pp. 33–77.

[10] P. E. Souganidis, Existence of Viscosity Solutions of Hamilton-Jacobi Equations, *J. Differential Equations*, Vol. **56**, 1985, pp. 345–390.

[11] P. E. Souganidis, Approximation Schemes for Viscosity Solutions of Hamilton-Jacobi Equations, *J. Differential Equations*, Vol. **59**, 1985, pp. 1–43.

[12] M. G. Crandall and P. L. Lions, Two Approximations of Solutions of Hamilton-Jacobi Equations, *Math. Comput.*, Vol. **43**, 1984, no. 167, pp. 1–19.

[13] L. C. Evans, *Partial Differential Equations*, Berkeley Mathematics Lecture Notes, Volume 3B, 1994.

[14] S. Osher and C. Shu, High-Order Essentially Nonoscillatory Schemes for Hamilton-Jacobi Equations, *SIAM J. Numer. Anal.*, Vol.**28**, No. 4, August 1991, pp. 907–922.

[15] W. K. Lyons, *The Single Conservation Law of Discontinuous Media*, Ph.D. Thesis, Brown University, 1980.